

Supplementary Figures for Biogeochemical impacts of tidally driven internal mixing in the Early Eocene

Jean-Baptiste Ladant¹, Jeanne Millot-Weil^{1,*}, Casimir de Lavergne², Mattias Green³,
Sébastien Nguyen¹, Yannick Donnadieu⁴

¹LSCE

²LOCEAN

³Bangor University

⁴CEREGE

Figures S1 – S12.

References.

M2 tidal dissipation

$\log_{10}(\text{W.m}^{-2})$

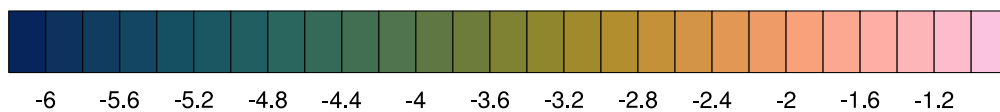
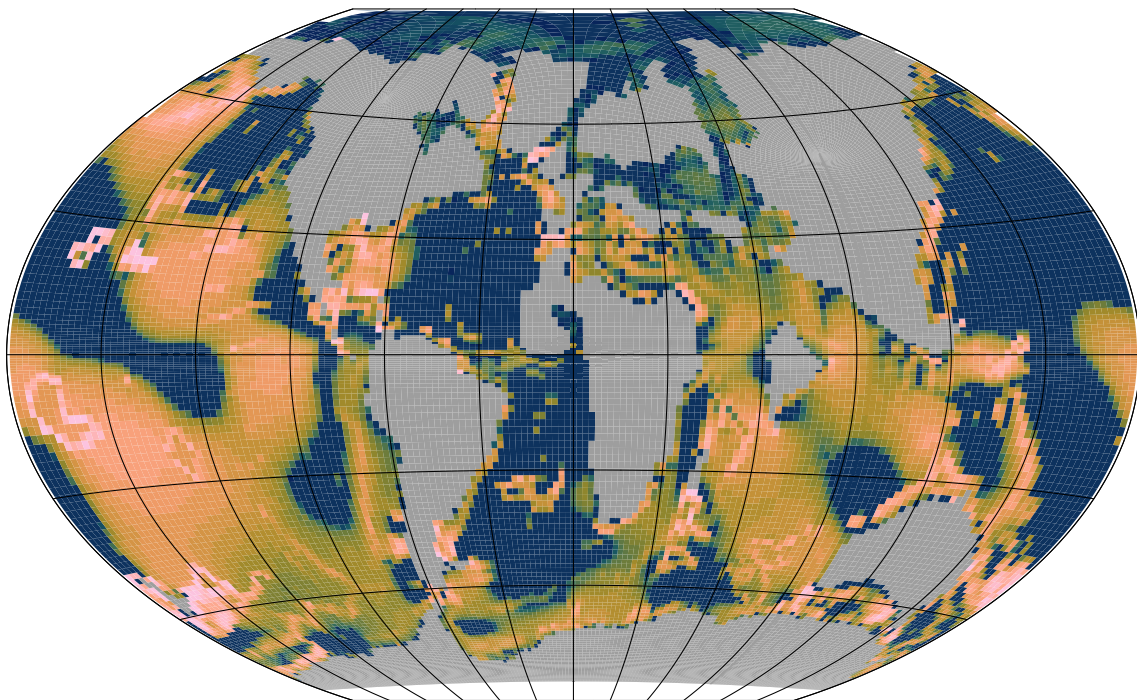


Figure S1. Early Eocene M2 tide dissipation rates from Green and Huber (2013) at model resolution.

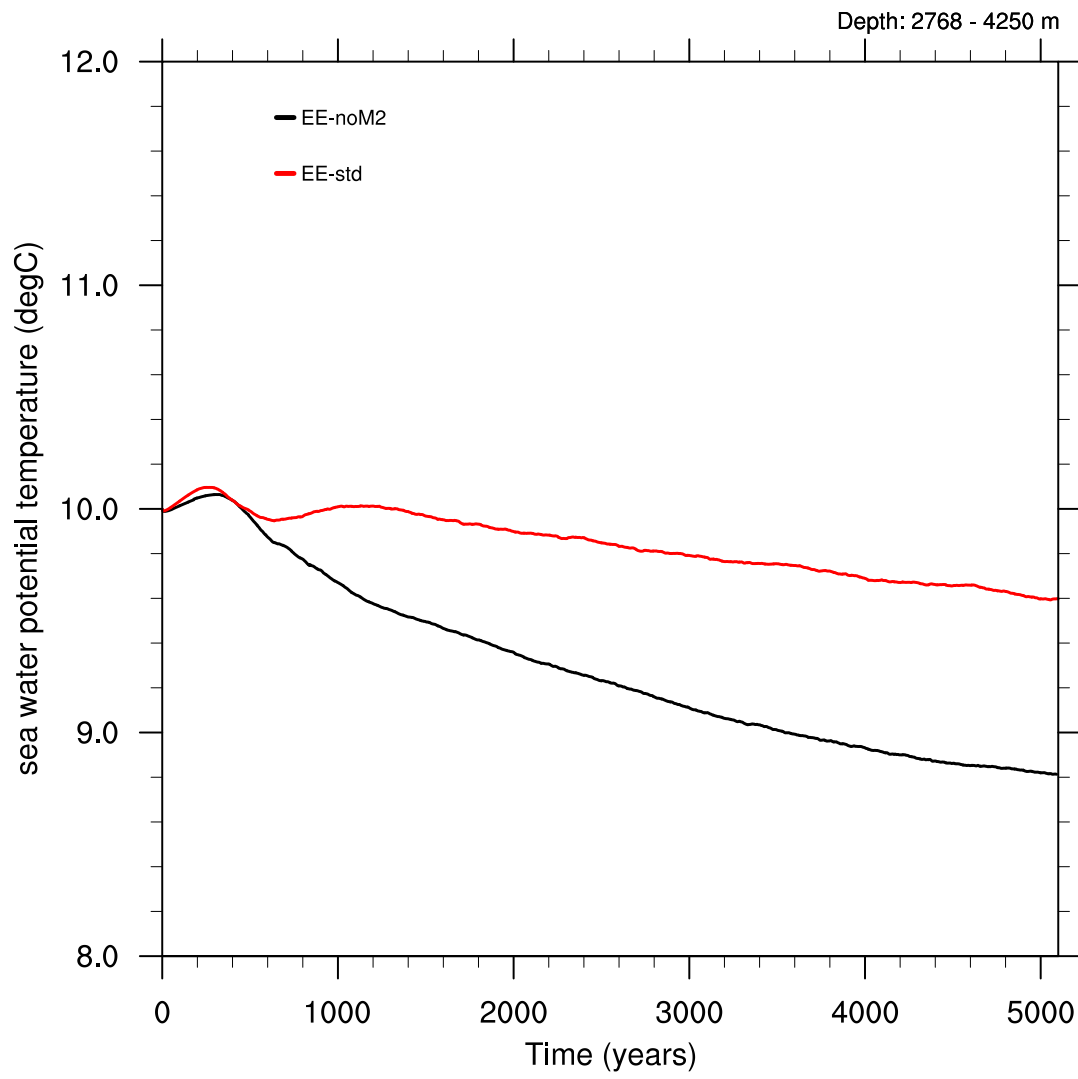


Figure S2. Timeseries of deep ocean temperatures for EE-noM2 (black) and EE-std (red).

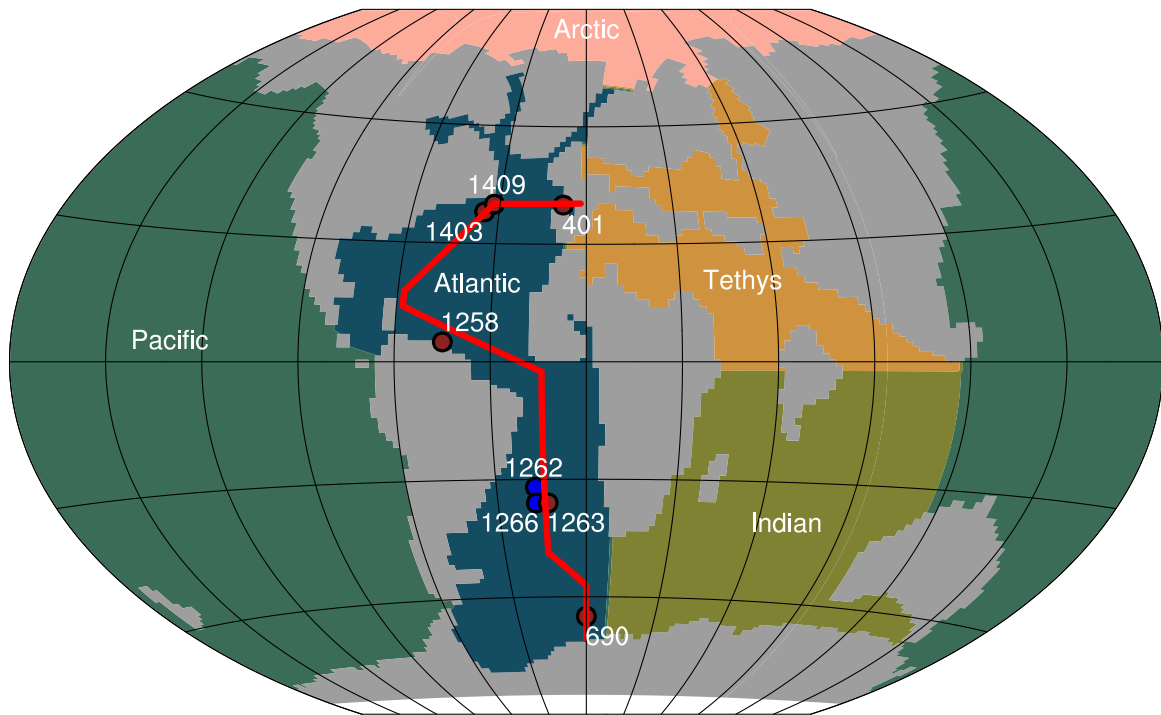


Figure S3. Ocean basins in the Early Eocene. The red contour is the Atlantic transect used in Figure 9. The locations of relevant sites are shown as well: ODP Site 690 (Zhou et al. 2014), ODP Sites 1262, 1263 and 1266 (Pälike et al. 2014, Zhou et al. 2014, Xue et al. 2022), ODP Site 1258 (Pälike et al. 2014), IODP Site 1403 and 1409 (Xue et al. 2023) and DSDP Site 401 (Pälike et al. 2014).

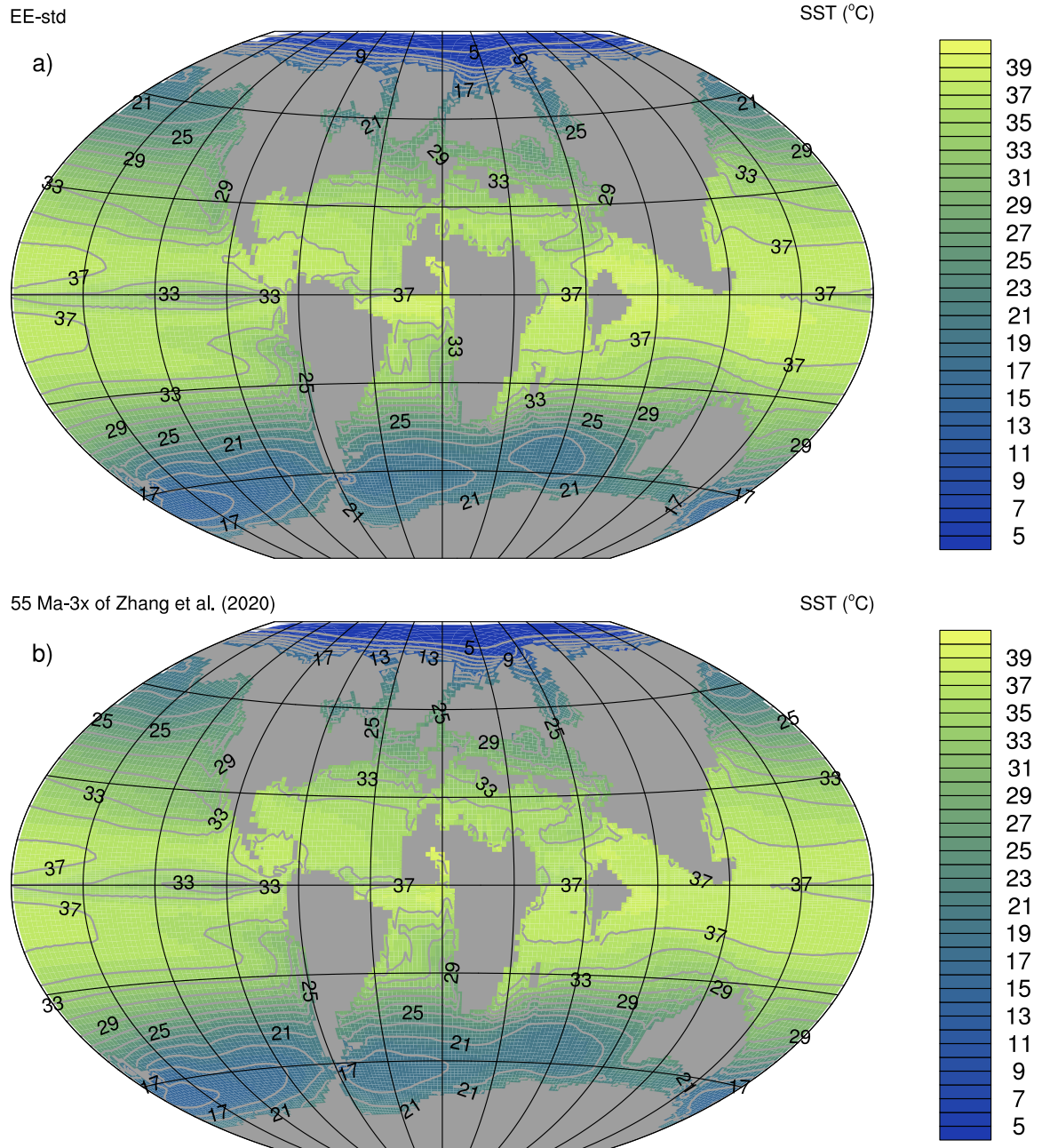


Figure S4. Summer sea surface temperature (°C) in (a) EE-std and (b) the 55 Ma-3x simulation of Zhang et al. (2020). We show summer SST, rather than annual mean, because this is what is presented on Fig. 2a of Zhang et al. (2020)(in contrast to what the legend of the figure reads in Zhang et al. (2020)).

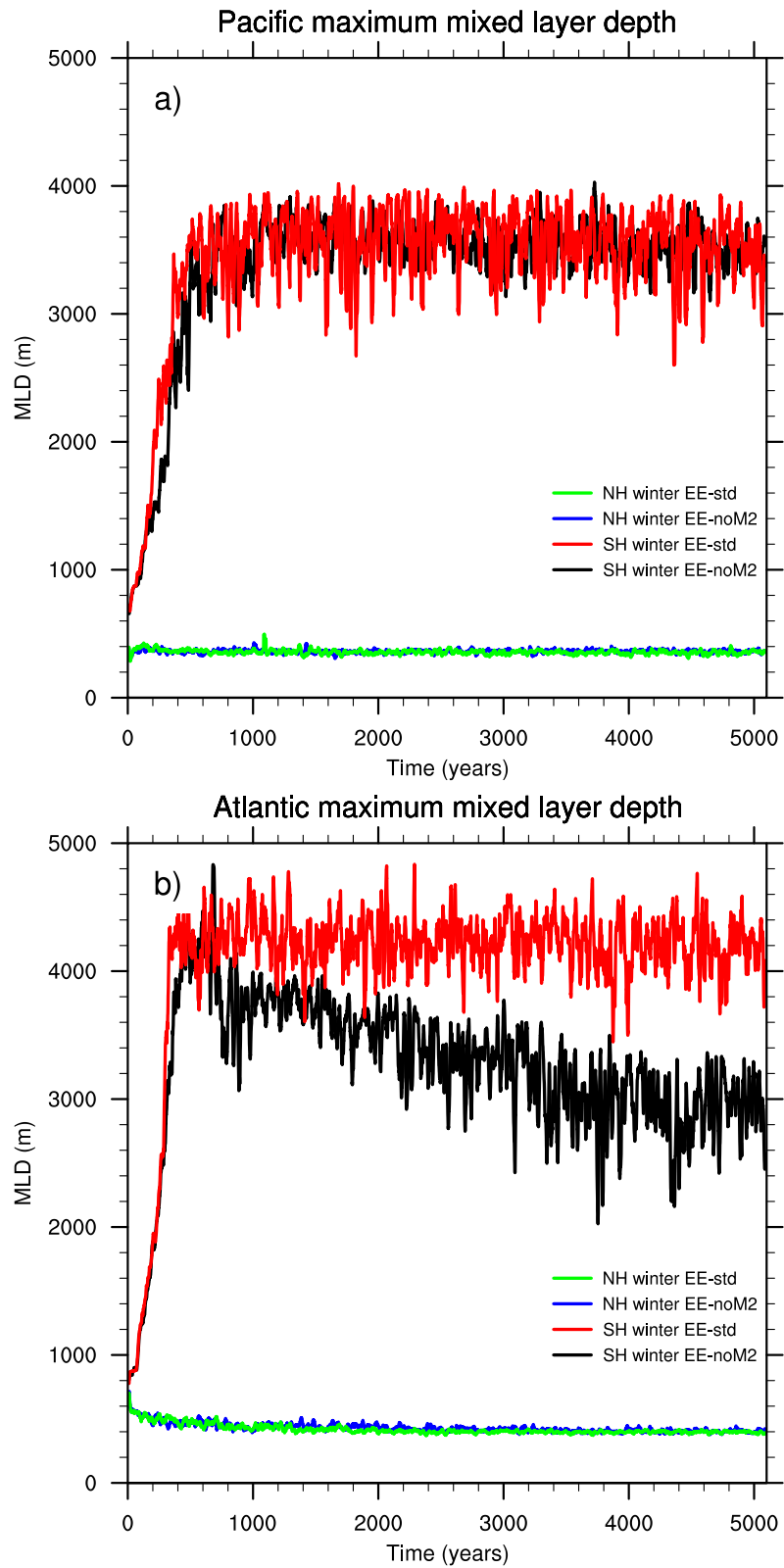


Figure S5. Timeseries of maximum winter mixed-layer depths (m) in the Atlantic and Pacific basin (Fig. S3). Black and red lines represent Southern Hemisphere MLD in EE-noM2 and EE-std respectively. Blue and green lines represent Northern Hemisphere MLD in EE-noM2 and EE-std respectively.

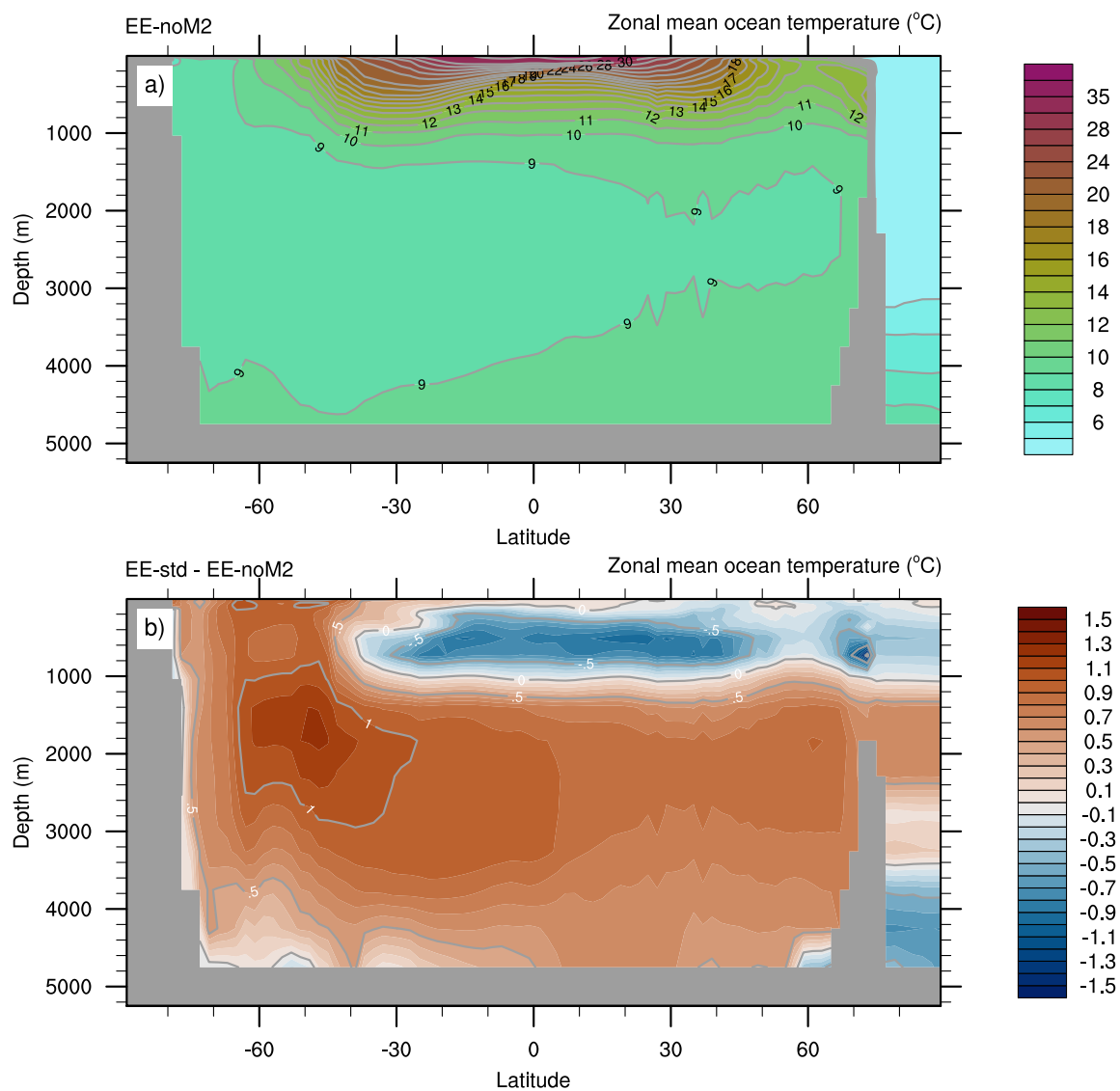


Figure S6. (a) Global zonal mean ocean temperature (°C) in EE-noM2. (b) Global zonal mean ocean temperature difference (°C) in EE-std relative to EE-noM2.

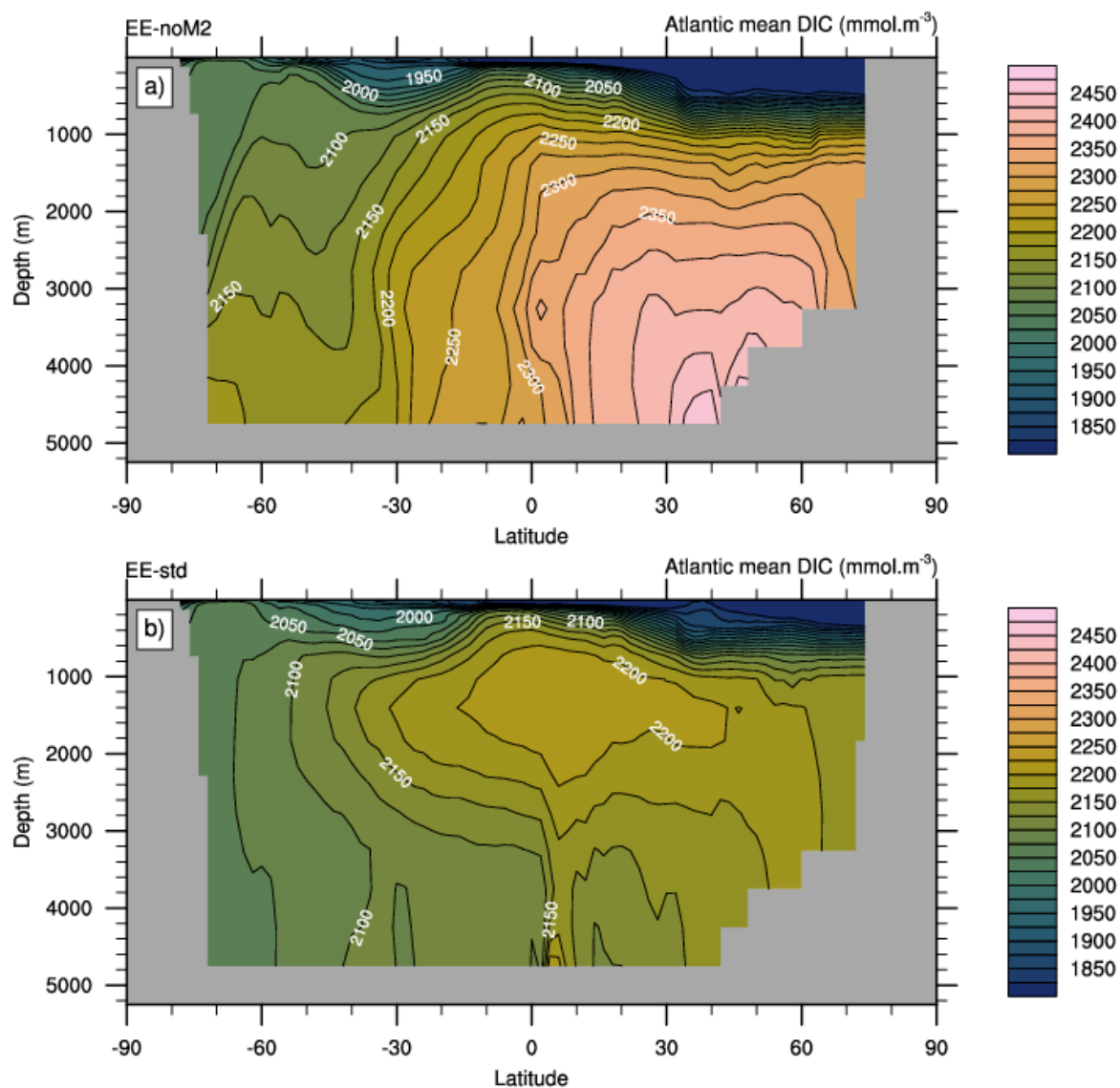


Figure S7. Zonally-averaged dissolved inorganic carbon concentrations (mmol.m⁻³) across the Atlantic in EE-noM2 (a) and EE-std (b).

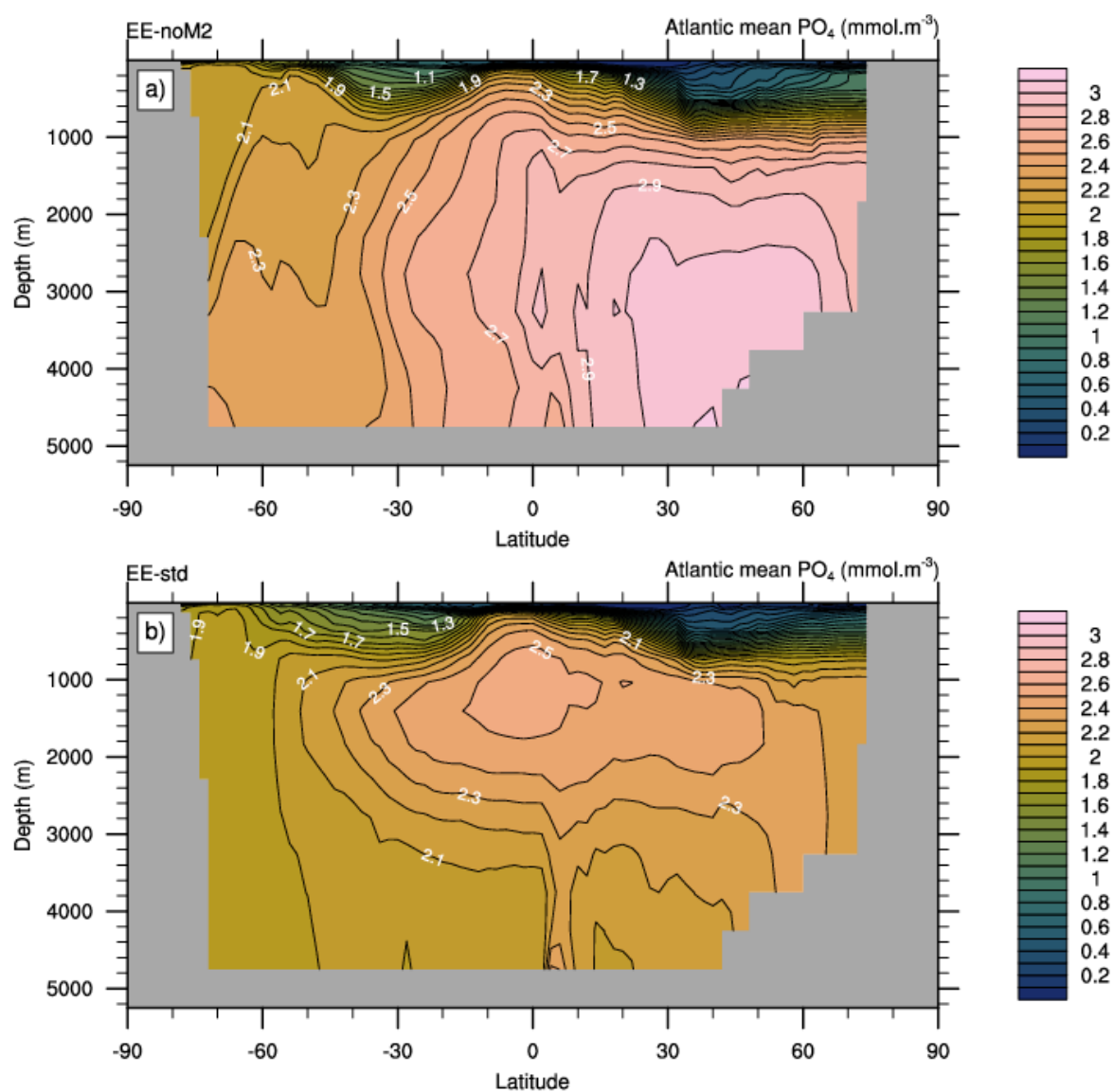


Figure S8. Zonally-averaged phosphate concentrations (mmol.m^{-3}) across the Atlantic in EE-noM2 (a) and EE-std (b).

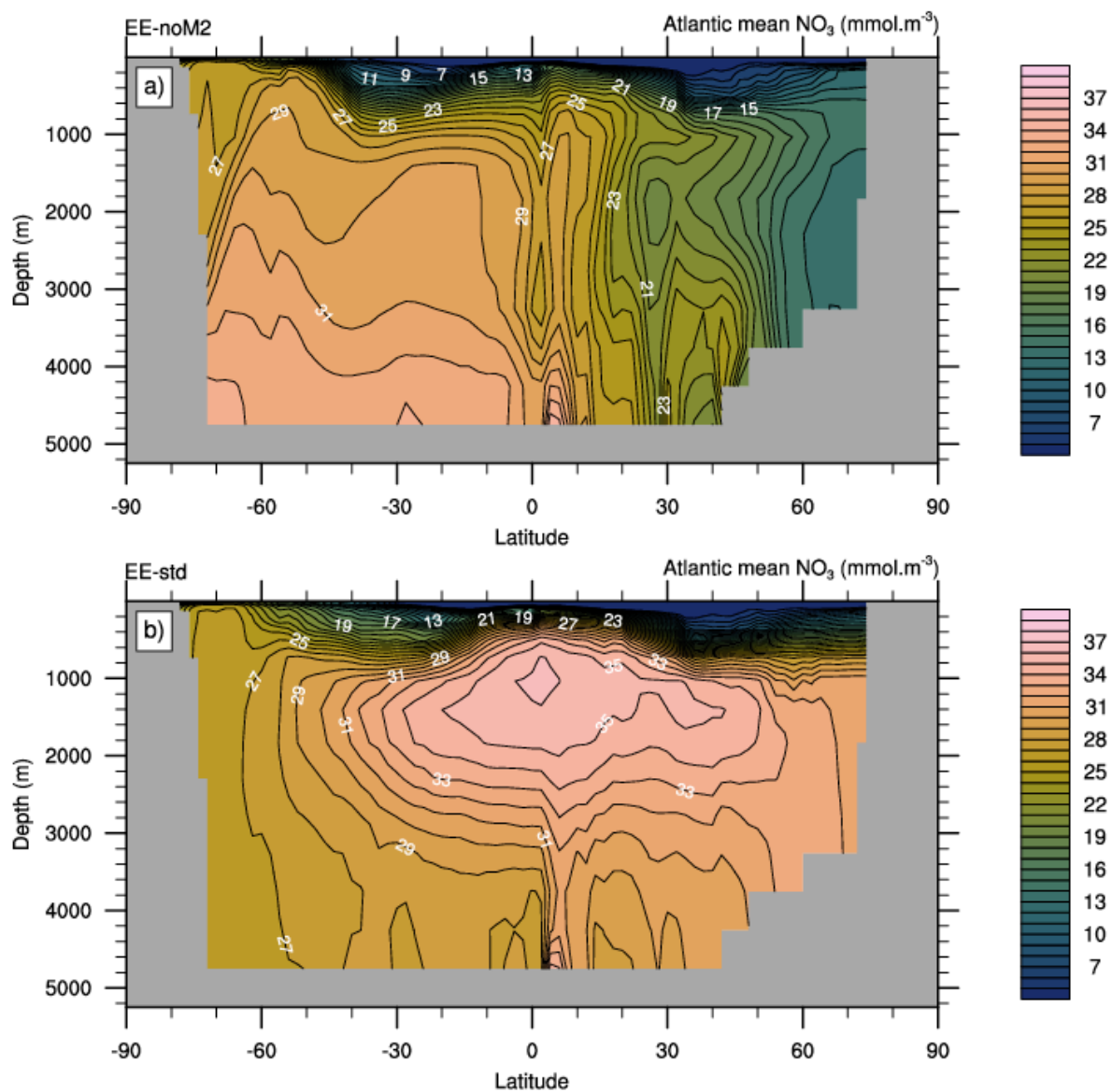


Figure S9. Zonally-averaged nitrate concentrations (mmol.m^{-3}) across the Atlantic in EE-noM2 (a) and EE-std (b).

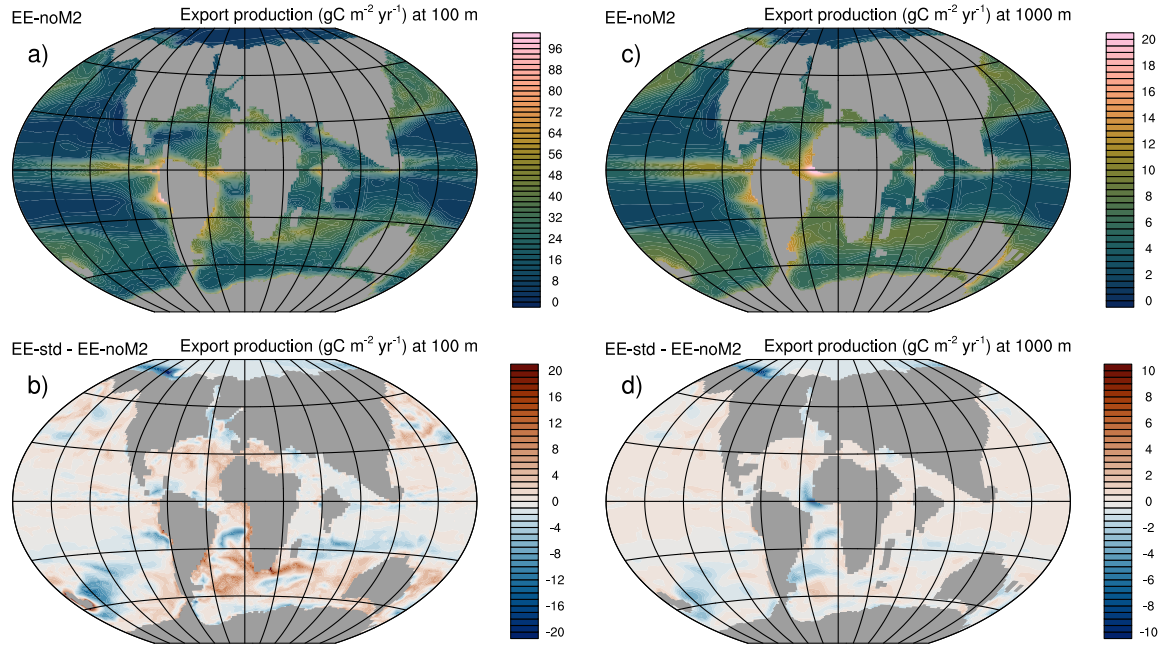


Figure S10. Export production ($\text{gC m}^{-2} \text{yr}^{-1}$) at 100 m (a) and 1000 m (c) in EE-noM2. Export production difference ($\text{gC m}^{-2} \text{yr}^{-1}$) at 100 m (b) and 1000 m (d) between EE-std and EE-noM2.

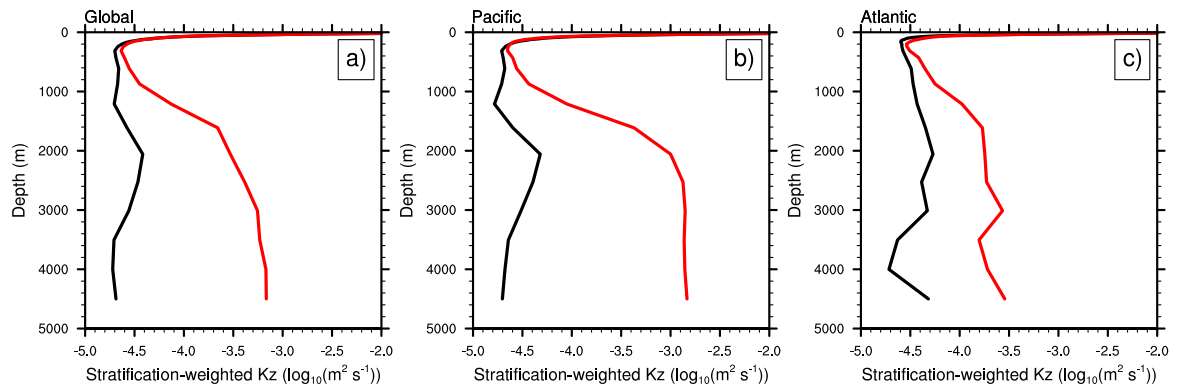


Figure S11. (a) Global, (b) Pacific and (c) Atlantic mean stratification-weighted vertical diffusivity ($\log(\text{m}^2 \text{s}^{-1})$) in EE-noM2 (black) and EE-std (red).

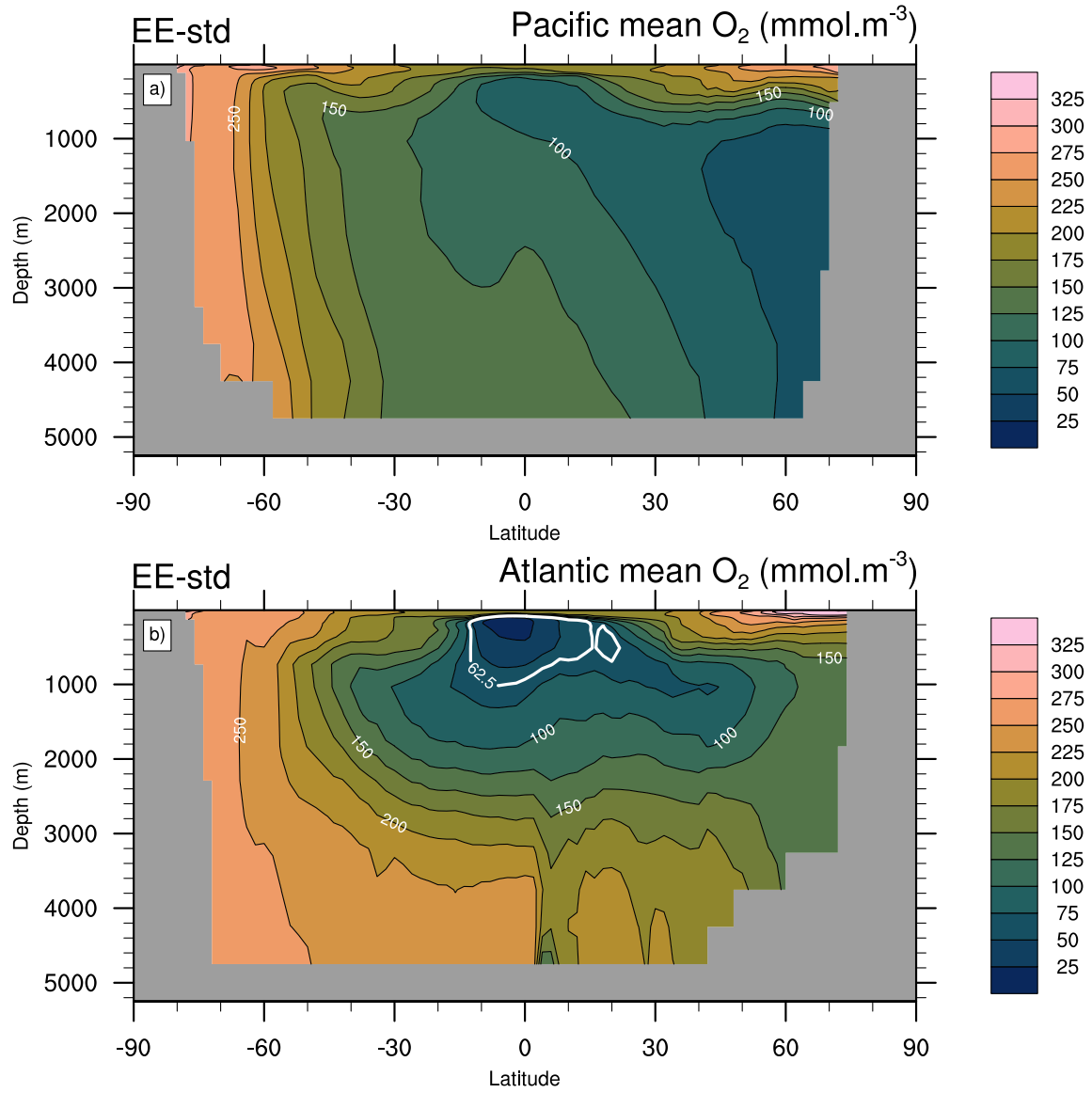


Figure S12. Zonally-averaged (a) Pacific and (b) Atlantic dissolved oxygen concentrations (mmol.m^{-3}) in EE-std. Panel (b) is identical to Fig. 6b.

References

Green, J.A.M., Huber, M., 2013. Tidal dissipation in the early Eocene and implications for ocean mixing. *Geophys. Res. Lett.* 40, 2707–2713. <https://doi.org/10.1002/grl.50510>

Pälike, C., Delaney, M.L., Zachos, J.C., 2014. Deep-sea redox across the Paleocene-Eocene thermal maximum. *Geochem. Geophys. Geosystems* 15, 1038–1053. <https://doi.org/10.1002/2013GC005074>

Xue, P., Chang, L., Dickens, G.R., Thomas, E., 2022. A Depth-Transect of Ocean Deoxygenation During the Paleocene-Eocene Thermal Maximum: Magnetofossils in Sediment Cores From the Southeast Atlantic. *J. Geophys. Res. Solid Earth* 127, e2022JB024714. <https://doi.org/10.1029/2022JB024714>

Xue, P., Chang, L., Thomas, E., 2023. Abrupt Northwest Atlantic deep-sea oxygenation decline preceded the Palaeocene-Eocene Thermal Maximum. *Earth Planet. Sci. Lett.* 618, 118304. <https://doi.org/10.1016/j.epsl.2023.118304>

Zhang, Y., Huck, T., Lique, C., Donnadieu, Y., Ladant, J.-B., Rabineau, M., Aslanian, D., 2020. Early Eocene vigorous ocean overturning and its contribution to a warm Southern Ocean. *Clim. Past* 16, 1263–1283. <https://doi.org/10.5194/cp-16-1263-2020>

Zhou, X., Thomas, E., Rickaby, R.E.M., Winguth, A.M.E., Lu, Z., 2014. I/Ca evidence for upper ocean deoxygenation during the PETM. *Paleoceanography* 29, 964–975. <https://doi.org/10.1002/2014PA002702>

Zhou, X., Thomas, E., Winguth, A.M.E., Ridgwell, A., Scher, H., Hoogakker, B.A.A., Rickaby, R.E.M., Lu, Z., 2016. Expanded oxygen minimum zones during the late Paleocene-early Eocene: Hints from multiproxy comparison and ocean modeling. *Paleoceanography* 31, 1532–1546. <https://doi.org/10.1002/2016PA003020>